

Graph Edit Distance from Spectral Seriation

Antonio Robles-Kelly and Edwin R. Hancock *

Abstract

This paper is concerned with computing graph edit distance. One of the criticisms that can be leveled at existing methods for computing graph edit distance is that they lack some of the formality and rigour of the computation of string edit distance. Hence, our aim is to convert graphs to string sequences so that string matching techniques can be used. To do this we use a graph spectral seriation method to convert the adjacency matrix into a string or sequence order. We show how the serial ordering can be established using the leading eigenvector of the graph adjacency matrix. We pose the problem of graph-matching as maximum a posteriori probability (MAP) alignment of the seriation sequences for pairs of graphs. This treatment leads to an expression in which the edit cost is the negative logarithm of the a posteriori sequence alignment probability. We compute the edit distance by finding the sequence of string edit operations which minimise the cost of the path traversing the edit lattice. The edit costs are determined by the components of the leading eigenvectors of the adjacency matrix, and by the edge densities of the graphs being matched. We demonstrate the utility of the edit-distance on a number of graph clustering problems.

1 Introduction

The quest for a robust means of inexact graph matching has been the focus of sustained activity in the areas of computer vision and structural pattern recognition for over two

*Department of Computer Science, The University of York, York, Y01 5DD, UK. email: {arobkell,erh}@cs.york.ac.uk

decades [34, 31, 10, 12, 44, 26]. Many different approaches have been adopted to the problem, including relaxation labelling [6, 11, 12, 44] and constraint satisfaction [35, 44, 4], structural pattern recognition (including the use of graph edit distance) [31, 10], information theoretic methods [26], and, graph-spectral methods [40, 22]. Each of these approaches has its merits. For instance, information theoretic methods [6, 44] are strongly principled since they model the graph-matching process using probability distributions. Matching by minimising edit distance [31, 10, 26] is attractive since it gauges the similarity of graphs by counting the number of structural modifications needed to make graphs isomorphic with one-another. Graph spectral methods are elegant because of their use of a matrix representation [40, 22]. However, there are weaknesses too. Information theoretic methods are limited by the fact that the required probability distributions can become difficult to construct and manipulate due the combinatorial nature of the underlying state-space. Of course this problem can be overcome to some extent by making simplifying assumptions. For instance, in relaxation labelling the complexity can be curbed by representing the distribution over edges or faces [6]. In order to overcome the computational problems associated with using discrete densities, Bagdanov and Worring [2] use normal distributions to model the distribution of the random variables in their first-order Gaussian graphs. These methods can lead to algorithms for learning graph prototypes from training data. In the case of graph edit-distance the costs of elementary edit operations must be set heuristically since no well-defined learning procedure exists, and moreover, the method lacks some of the formal underpinning of string edit distance. Graph-spectral methods can be fragile to structural error [40] unless expensive iterative methods are adopted [22].

The aim in this paper is to exploit some of the strengths of the methods listed above, while overcoming their weaknesses. The overall aim is to use a spectral representation, and to pose the computation of graph edit distance in a probabilistic setting. This work is timely for a number of reasons. First, there has recently been renewed interest in the problem of computing graph edit distance. For instance, Bunke and his co-workers have returned to the problem and have shown a relationship between graph edit distance and the size of the maximum common subgraph [3]. Second, graph spectral methods have been shown to work

effectively if either a careful choice of representation is made, or if they are combined with statistical methods. For instance, Shokoufandeh *et al* [36] have shown how to index shock trees using an eigenvalue interleaving theorem, and Luo and Hancock [22] have shown how Umeyama’s [40] matrix factorisation method can be rendered robust to structural error using the apparatus of the EM algorithm. However, despite this progress it is clear that there is still much remaining to be done on the convergence of structural, spectral and statistical methods.

1.1 Motivation

One way of overcoming the problems listed above is to use graph-spectral methods to convert graphs to string sequences and to use probabilistic methods to measure the similarity of the sequences, and hence compute graph edit distance. We have already performed an initial study of this problem [29]. Here we made use of the relationship between the leading eigenvector of the row-normalised adjacency matrix and the steady state random walk on the associated graph. The string sequence is defined by the state probabilities of the random walk after an infinite number of time steps. Edit distance computation is based on a set of heuristic elementary costs. However, the string sequence delivered by the steady state site probabilities is not guaranteed to be edge connected, and hence in comparing the strings information concerning the structure of the graph is discarded. This paper takes this work further by casting the problem of recovering an edge connected path sequence in a more explicit energy minimisation setting, and, by casting the problems of computing edit costs and string matching in a probabilistic setting.

To meet the goals listed above, in this paper we aim to recover a string in which the node sequence order maximally preserves edge connectivity constraints. More specifically, we are interested in the task of ordering the set of nodes in a graph in a sequence such that strongly correlated nodes are placed next to one another. This problem is known as seriation and is important in a number of areas including data visualisation and bioinformatics, where it is used for DNA sequencing. The seriation problem can be approached in a number of ways. Clearly the problem of searching for a serial ordering of the nodes, which maximally preserves

the edge ordering is one of exponential complexity. As a result approximate solution methods have been employed. These involve casting the problem in an optimisation setting. Hence techniques such as simulated annealing and mean field annealing have been applied to the problem [33, 37]. It may also be formulated using semidefinite programming [17], which is a technique closely akin to spectral graph theory since it relies on eigenvector methods. However, recently Atkins, Boman and Hendrikson [1] have shown how to use an eigenvector of the Laplacian matrix to sequence relational data. There is an obvious parallel between this method and the use of eigenvector methods to locate steady state random walks on graphs [25, 20].

Hence, we aim to exploit this seriation technique to develop a spectral method for computing graph edit distance. The task of posing the inexact graph matching problem in a matrix setting has proved to be an elusive one. This is disappointing since a rich set of potential tools are available from the field of mathematics referred to as spectral graph theory. This is the term given to a family of techniques that aim to characterise the global structural properties of graphs using the eigenvalues and eigenvectors of the adjacency matrix [7]. In the computer vision literature there have been a number of attempts to use spectral properties for graph-matching, object recognition and image segmentation. Umeyama has an eigendecomposition method that matches graphs of the same size [40]. Borrowing ideas from structural chemistry, Scott and Longuet-Higgins were among the first to use spectral methods for correspondence analysis [32]. They showed how to recover correspondences via singular value decomposition on the point association matrix between different images. In keeping more closely with the spirit of spectral graph theory, Shapiro and Brady [35] developed an extension of the Scott and Longuet-Higgins method, in which point sets are matched by comparing the eigenvectors of the point proximity matrix. Horaud and Sossa [15] have adopted a purely structural approach to the recognition of line-drawings. Their representation is based on the immanental polynomials for the Laplacian matrix of the line-connectivity graph. Shokoufandeh, Dickinson and Siddiqi [36] have shown how graphs can be encoded using local topological spectra for shape recognition from large databases. In a recent paper, Luo and Hancock [22] have returned to the method of Umeyama [40] and

have shown how it can be rendered robust to differences in graph-size and structural errors. Commencing from a Bernoulli distribution for the correspondence errors, they develop an expectation maximisation algorithm for graph-matching. Correspondences are recovered in the M or maximisation step of the algorithm by performing singular value decomposition on the weighted product of the adjacency matrices for the graphs being matched. The correspondence weight matrix is updated in the E or expectation step. However, since it is iterative the method is relatively slow and is sensitive to initialisation.

1.2 Contribution

We pose the recovery of the seriation path as that of finding an optimal permutation order subject to edge connectivity constraints. By using the Perron-Frobenius theorem [41], we show that the optimal permutation order is given by the leading eigenvector of the adjacency matrix. The seriation path may be obtained from this eigenvector using a simple edge-filtering technique. By using the spectral seriation method, we are able to convert the graph into a string. This opens up the possibility of performing graph matching by performing string alignment. We pose the problem as maximum a posteriori probability estimation of an optimal alignment sequence on an edit lattice by minimising the Levenshtein or edit distance [19, 42]. The edit distance is the negative log-likelihood of the a posteriori alignment probability. To compute the alignment probability, we require two model ingredients. The first of these is an edge compatibility measure for the edit sequence. We use a simple error model to show how these compatibilities may be computed using the edge densities for the graphs under match. The second model ingredient is a set of node correspondence probabilities. We model these using a Gaussian distribution on the components of the leading eigenvectors of the adjacency matrices. We can follow Wagner [42] and use dynamic programming to evaluate the edit distance between strings and hence recover correspondences. It is worth stressing that although there have been attempts to extend the string edit idea to trees and graphs [31, 34], there is considerable current effort aimed at putting the underlying methodology on a rigorous footing.

2 Graph Seriation

Consider the undirected graph $G = (V, E)$ with node index-set V and edge-set $E \subseteq V \times V$. Associated with the graph is a symmetric adjacency matrix A whose elements are defined as follows

$$A(j, k) = \begin{cases} 1 & \text{if } (j, k) \in E \\ 0 & \text{otherwise} \end{cases} \quad (1)$$

Our aim is to assign the nodes of the graph to a sequence order which preserves the edge ordering of the nodes. This sequence can be viewed as an edge connected path on the graph. Let the path commence at the node j_1 and proceed via the sequence of edge-connected nodes $X = \{j_1, j_2, j_3, \dots\}$ where $(j_i, j_{i+1}) \in E$. With these ingredients, the problem of finding the path can be viewed as one of seriation, subject to edge connectivity constraints.

The seriation problem as stated by Atkins, Boman and Hendrickson [1] is as follows. The aim is to find a path sequence for the nodes in the graph using a permutation π . The required permutation is sought so as to minimise the penalty function

$$g(\pi) = \sum_{i=1}^{|V|} \sum_{j=1}^{|V|} A(i, j) (\pi(i) - \pi(j))^2$$

Unfortunately, minimising $g(\pi)$ is potentially NP complete due to the combinatorial nature of the discrete permutation π . To overcome this problem, a relaxed solution is sought that approximates the structure of $g(\pi)$ using a vector $\vec{x} = (x_1, x_2, \dots)$ of continuous variables x_i . Hence, the penalty function considered is

$$\hat{g}(\vec{x}) = \sum_{i=1}^{|V|} \sum_{j=1}^{|V|} A(i, j) (x_i - x_j)^2$$

The value of $\hat{g}(\vec{x})$ does not change if a constant amount is added to each of the components x_i . Hence, the minimisation problem must be subject to constraints on the components of the vector \vec{x} . The constraints are that

$$\sum_{i=1}^{|V|} x_i^2 = 1 \quad \text{and} \quad \sum_{i=1}^{|V|} x_i^2 \neq 0 \quad (2)$$

Atkins, Bowman and Atkinson show that the solution to this relaxed problem may be obtained from the Fiedler vector of the Laplacian matrix $L = D - A$, where D is the diagonal

degree matrix with elements $D(i, i) = \sum_{j=1}^{|V|} A(i, j)$ equal to the total weight of the edges connected to the node i .

Unfortunately, the procedure described above does not meet our requirements since the penalty function $\hat{g}(\vec{x})$, does not impose edge connectivity constraints on the ordering computed during the minimisation process. To overcome this shortcoming, we turn our attention instead to maximising the cost function

$$\hat{g}_E(\vec{x}) = \sum_{i=1}^{|V|-1} \sum_{k=1}^{|V|} (A(i, k) + A(i + 1, k)) x_k^2 \quad (3)$$

When we combine the modified cost function with the constraints, we have that

$$\sum_{i=1}^{|V|-1} \sum_{k=1}^{|V|} (A(i, k) + A(i + 1, k)) x_k^2 = \lambda \sum_{i=1}^{|V|-1} (x_i^2 + x_{i+1}^2) \quad (4)$$

By introducing the matrix

$$\Omega = \begin{bmatrix} 1 & 0 & 0 & 0 & \dots & 0 \\ 0 & 2 & 0 & 0 & \dots & 0 \\ 0 & 0 & 2 & 0 & \dots & 0 \\ \vdots & \vdots & \ddots & \ddots & \ddots & \vdots \\ 0 & 0 & \dots & 0 & 2 & 0 \\ 0 & 0 & \dots & 0 & 0 & 1 \end{bmatrix} \quad (5)$$

we can make the path connectivity requirement more explicit, and the maximiser of $g_E(\vec{x})$ satisfies the condition

$$\lambda = \arg \max_{x_*} \frac{\vec{x}_*^T \Omega A \vec{x}_*}{\vec{x}_*^T \Omega \vec{x}_*} \quad (6)$$

As a result, the leading eigenvalue λ_* of the adjacency matrix A is the maximiser of the cost function $\hat{g}_E(\vec{x})$. From the Perron-Frobenius theorem [41], it is known that the maximiser of this utility function is the leading (left) eigenvector of the matrix A . Moreover, since A is a real positive definite symmetric matrix, the associated eigenvector ϕ^* is unique. The Perron-Frobenius theorem ensures that the maximum eigenvalue $\lambda_* > 0$ of A has multiplicity one and, moreover, the coefficients of the corresponding eigenvector ϕ^* are all positive. As a result the remaining eigenvectors of A have at least one negative coefficient

and one positive coefficient. If A is substochastic, ϕ^* is also known to be linearly independent of the all-ones vector \mathbf{e} .

The elements of the leading eigenvector ϕ^* can be used to construct a serial ordering of the nodes in the graph. We commence from the node associated with the largest component of ϕ^* . We then sort the elements of the leading eigenvector such that they are both in the decreasing magnitude order of the coefficients of the eigenvector, and satisfy edge connectivity constraints on the graph. The procedure is a recursive one that proceeds as follows. At each iteration, we maintain a list of nodes visited. At iteration k let the list of nodes be denoted by \mathcal{L}_k . Initially, $\mathcal{L}_1 = j_1$ where $j_1 = \arg \max_j \phi^*(j)$, i.e. j_1 is the component of ϕ^* with the largest magnitude. Next, we search through the set of first neighbours $\mathcal{N}_{j_1} = \{k | (j_1, k) \in E\}$ of j_1 to find the node associated with the largest remaining component of ϕ^* . The second element in the list is $j_2 = \arg \max_{l \in \mathcal{N}_{j_1}} \phi^*(l)$. The node index j_2 is appended to the list of nodes visited and the result is \mathcal{L}_2 . In the k th (general) step of the algorithm we are at the node indexed j_k and the list of nodes visited by the path so far is \mathcal{L}_k . We search through those first-neighbours of j_k that have not already been traversed by the path. The set of nodes is $C_k = \{l | l \in \mathcal{N}_{j_k} \wedge l \notin \mathcal{L}_k\}$. The next site to be appended to the path list is therefore $j_{k+1} = \arg \max_{l \in C_k} \phi^*(l)$. This process is repeated until no further moves can be made. This occurs when $C_k = \emptyset$ and we denote the index of the termination of the path by T . The serial ordering of the nodes of the graph X is given by the ordered list or string of node indices \mathcal{L}_T . Hence, the path commences at the node with the highest ranked eigenvector component, and then proceeds in an edge connected manner through the sequence of nodes that minimise the difference in the components of the eigenvector.

Figure 1 illustrates the seriation method on a simple graph. The left-hand panel shows the original graph with numeric labels assigned to the nodes. In the centre-panel we show the components of the leading eigenvector of the adjacency matrix, ordered according the numeric order of the node-labels. In the right-hand panel, we show the seriation path. This commences at the centre of the graph, and then moves around the perimeter.

There are similarities between the use of the leading eigenvector for seriation and the use of spectral methods to find the steady state random walk on a graph. There are more

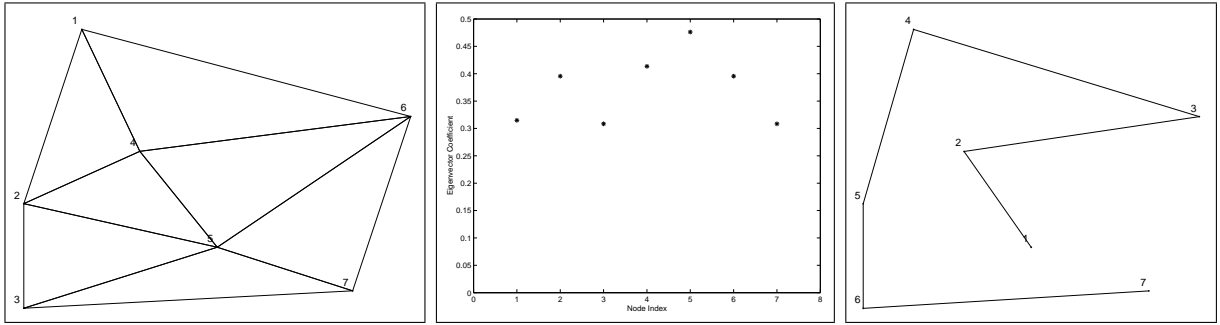


Figure 1: Left-hand panel: example graph; Middle panel: corresponding leading eigenvector; Right-hand panel: seriation results.

detailed discussions of the problem of locating the steady state random walk on a graph in the reviews by Lovasz [20] and Mohar [25]. An important result described in these papers, is that if we visit the nodes of the graph in the order defined by the magnitudes of the coefficients of the leading eigenvector of the transition probability matrix, then the path is the steady state Markov chain. In a recent paper [29], which represents the starting point which lead us to the research reported here, we have used the rank order of the steady state node visitation probabilities to define a string order. However, this path is not guaranteed to be edge connected. Hence, it can not be used to impose a string ordering on the nodes of a graph that encompasses edge-constraints. The seriation approach adopted in this paper does, on the other hand, impose edge connectivity constraints and can hence be used to convert graphs to strings in a manner which is suitable for computing edit distance.

3 Probabilistic Framework

We are interested in computing the edit distance between the graphs $G_M = (V_M, E_M)$ referred to as the model graph and the graph $G_D = (V_D, E_D)$ referred to as the data-graph. The leading eigenvectors of the adjacency matrices A_M for the graph G_M and A_D for the graph G_D are respectively ϕ_M^* and ϕ_D^* . The seriations of the two graphs generated from the leading eigenvectors are denoted by $X = \{x_1, x_2, \dots, x_{|V_M|}\}$ for the model graph and $Y = \{y_1, y_2, \dots, y_{|V_D|}\}$ for the data graph. These two strings are used to index the

rows and columns of an edit lattice. The rows of the lattice are indexed using the data-graph string, while the columns are indexed using the model-graph string. To allow for differences in the sizes of the graphs we introduce a null symbol ϵ which can be used to pad the strings. We pose the problem of computing the edit distance as that of finding a path $\Gamma = \langle \gamma_1, \gamma_2, \dots, \gamma_k, \dots, \gamma_L \rangle$ through the lattice. Each element $\gamma_k \in (V_D \cup \epsilon) \times (V_M \cup \epsilon)$ of the edit path is a Cartesian pair. We constrain the path to be connected on the edit lattice. In particular, the transition on the edit lattice from the state γ_k to the state γ_{k+1} is constrained to move in a direction that is increasing and connected in the horizontal, vertical or diagonal direction on the lattice. The diagonal transition corresponds to the match of an edge of the data graph to an edge of the model graph. A horizontal transition means that the data-graph index is not incremented, and this corresponds to the case where the traversed nodes of the model graph are null-matched. Similarly when a vertical transition is made, then the traversed nodes of the data-graph are null-matched.

Suppose that $\gamma_k = (a, b)$ and $\gamma_{k+1} = (c, d)$ represent adjacent states in the edit path between the serializations X and Y . According to the classical approach [42], the cost of the edit path is given by the sum of the costs of the elementary edit operations

$$d(X, Y) = C(\Gamma) = \sum_{\gamma_k \in \Gamma} \eta(\gamma_k \rightarrow \gamma_{k+1}) \quad (7)$$

where $\eta(\gamma_k \rightarrow \gamma_{k+1})$ is the cost of the transition between the states $\gamma_k = (a, b)$ and $\gamma_{k+1} = (c, d)$. The optimal edit path is the one that minimises the edit distance between the strings, and satisfies the condition $\Gamma^* = \arg \min_{\Gamma} C(\Gamma)$, and the edit distance is $d(X, Y) = C(\Gamma^*)$. Classically, the optimal edit sequence may be found using Dijkstra's algorithm [8] or by using the quadratic programming method of Wagner and Fisher [42]. However, there are two reasons why the classical string edit distance does not meet our needs in this paper. First, the edit costs need to reflect the string encoding of graph structure. In other words, the transitions on the edit lattice must take into account whether edge structure is being matched in a consistent manner. Second, we would like to cast the problem of minimum edit distance matching in a probabilistic setting so that we can develop statistical models for the costs on the edit lattice. In particular, we would like to do this in a manner which separates

the costs of visiting individual sites on the lattice and of making transitions between sites. In this way we can separate the role of evidence, i.e. the components of the leading eigenvectors, and constraints, i.e. whether edges are matched consistently.

Rather than commencing from an expression for the edit-cost, in this paper we pose the problem of recovering the optimal edit sequence as one of maximum a posteriori probability estimation. We aim to find the edit path that has maximum probability given the available leading eigenvectors of the data-graph and model-graph adjacency matrices. Hence, the optimal path is the one that satisfies the condition $\Gamma^* = \arg \max_{\Gamma} P(\Gamma | \phi_X^*, \phi_Y^*)$.

To develop this decision criterion into a practical edit distance computation scheme, we need to develop the *a posteriori* probability appearing above. We commence by using the definition of conditional probability to re-write the *a posteriori* path probability in terms of the joint probability density $P(\phi_X^*, \phi_Y^*)$ for the leading eigenvectors and the joint density function $P(\phi_X^*, \phi_Y^*, \Gamma)$ for the leading eigenvectors and the edit path. The result is

$$P(\Gamma | \phi_X^*, \phi_Y^*) = \frac{P(\phi_X^*, \phi_Y^*, \Gamma)}{P(\phi_X^*, \phi_Y^*)} \quad (8)$$

We can rewrite the joint density appearing in the numerator to emphasise and make explicit both the role of the components of the adjacency matrix leading eigenvectors and the component edit transitions. In this form

$$P(\Gamma | \phi_X^*, \phi_Y^*) = \frac{P(\phi_X^*(1), \phi_X^*(2), \dots, \phi_Y^*(1), \phi_Y^*(2), \dots, \gamma_1, \gamma_2, \dots)}{P(\phi_X^*, \phi_Y^*)} \quad (9)$$

To simplify the numerator, we make a conditional independence assumption. Specifically, we assume that the components $\phi_X^*(a)$ and $\phi_Y^*(b)$ of the leading eigenvectors of the model and data-graph adjacency matrices, depend only on the edit transition $\gamma_k = (a, b)$ associated with their node-indices. Using the chain-rule for conditional probability we can perform the factorisation

$$\frac{P(\phi_X^*(1), \phi_X^*(2), \dots, \phi_Y^*(1), \phi_Y^*(2), \dots, \gamma_1, \gamma_2, \dots)}{P(\phi_X^*, \phi_Y^*)} = \left\{ \prod_{k=1}^L P(\phi_X^*(a), \phi_Y^*(b) | \gamma_k) \right\} P(\gamma_1, \gamma_2, \dots, \gamma_L)$$

and as a result

$$P(\Gamma | \phi_X^*, \phi_Y^*) = \frac{\left\{ \prod_{k=1}^L P(\phi_X^*(a), \phi_Y^*(b) | \gamma_k) \right\} P(\gamma_1, \gamma_2, \dots, \gamma_L)}{P(\phi_X^*, \phi_Y^*)} \quad (10)$$

where $P(\gamma_1, \gamma_2, \dots, \gamma_L)$ is the joint prior for the sequence of edit transitions. To simplify the joint prior, we commence by applying the chain-rule of conditional probability

$$P(\gamma_1, \gamma_2, \dots, \gamma_L) = P(\gamma_1|\gamma_2, \dots, \gamma_L)P(\gamma_2|\gamma_3, \dots, \gamma_L) \dots P(\gamma_k|\gamma_{k+1}, \dots, \gamma_L) \dots P(\gamma_{L-1}|\gamma_L)P(\gamma_L) \quad (11)$$

To simplify this factorisation we assume that the sites on the edit lattice are conditionally dependant only on those that are immediate neighbours. As a result $P(\gamma_k|\gamma_{k+1}, \dots, \gamma_L) = P(\gamma_k|\gamma_{k+1})$. Hence, we can write

$$P(\gamma_1, \gamma_2, \dots, \gamma_L) = P(\gamma_L) \prod_{k=1}^{L-1} P(\gamma_k|\gamma_{k+1}) \quad (12)$$

This takes the form of a factorisation of conditional probabilities for transitions between sites on the edit lattice $P(\gamma_k|\gamma_{k+1})$, except for the term $P(\gamma_L)$ which results from the final site visited on the lattice. To arrive at a more homogeneous expression, we use the definition of conditional probability to re-express the joint conditional measurement density for the adjacency matrix leading eigenvectors in the following form

$$P(\phi_X^*(a), \phi_Y^*(b)|\gamma_k) = \frac{P(\gamma_k|\phi_X^*(a), \phi_Y^*(b))P(\phi_X^*(a), \phi_Y^*(b))}{P(\gamma_k)} \quad (13)$$

Substituting Equations (12) and (13) into Equation (10) we find

$$P(\Gamma|\phi_X^*, \phi_Y^*) = \left\{ \prod_{k=1}^L P(\gamma_k|\phi_X^*(a), \phi_Y^*(b)) \frac{P(\gamma_k, \gamma_{k+1})}{P(\gamma_k)P(\gamma_{k+1})} \right\} \frac{\prod_{k=1}^L P(\phi_X^*(a), \phi_Y^*(b))}{P(\phi_X^*, \phi_Y^*)}$$

Since, the joint measurement density $P(\phi_X^*, \phi_Y^*)$ does not depend on the edit path, it does not influence the decision process, and we remove it from further consideration. Hence, the optimal path across the edit lattice is

$$\Gamma^* = \arg \max_{\gamma_1, \gamma_2, \dots, \gamma_L} \left\{ \prod_{k=1}^L P(\gamma_k|\phi_X^*(a), \phi_Y^*(b)) \frac{P(\gamma_k, \gamma_{k+1})}{P(\gamma_k)P(\gamma_{k+1})} \right\} \quad (14)$$

The information concerning the structure of the edit path on the lattice is captured by the quantity

$$R_{k,k+1} = \frac{P(\gamma_k, \gamma_{k+1})}{P(\gamma_k)P(\gamma_{k+1})} \quad (15)$$

We refer to this quantity as the edge-compatibility coefficient.

To establish a link with the classical edit distance picture presented earlier, we can re-express the location of the optimal edit path as an minimisation problem involving the negative logarithm of the *a posteriori* path probability. The optimal path is the one that satisfies the condition

$$\Gamma^* = \arg \min_{\gamma_1, \gamma_2, \dots, \gamma_L} \left\{ \sum_{k=1}^L \left[-\ln P(\gamma_k | \phi_X^*(a), \phi_Y^*(b)) - \ln R_{k,k+1} \right] \right\} \quad (16)$$

As a result the elementary edit cost $\eta(\gamma_k \rightarrow \gamma_{k+1})$ associated with the transition from the site $\gamma_k = (a, b)$ to the site $\gamma_{k+1} = (c, d)$ is

$$\eta(\gamma_k \rightarrow \gamma_{k+1}) = -\left(\ln P(\gamma_k | \phi_X^*(a), \phi_Y^*(b)) + \ln P(\gamma_{k+1} | \phi_X^*(c), \phi_Y^*(d)) + \ln R_{k,k+1} \right) \quad (17)$$

The expression hence contains separate terms associated with the cost of visiting individual sites on the lattice, and for making transitions between sites. The cost of visiting the sites depends only on the components of the eigenvectors, and reflects the raw measurement data available to the graph matching method. The transition between sites, on the other hand, depends on whether there is consistent connecting edge structure between the sites on the edit lattice.

4 Model Ingredients

To compute the edit costs, we require models of the *a posteriori* probabilities of visiting the sites of the edit lattice, i.e. $P(\gamma_k | \phi_X^*(a), \phi_Y^*(b))$ and of $R_{k,k+1}$.

4.1 Lattice Transition Probabilities

The edge compatibility coefficient $R_{k,k+1}$ can be modelled using a simple model of node attendance [43]. We assume that there is a uniform probability p that individual nodes, in either of the graphs being matched, are missing due to the action of detection errors. These errors may be due to a number of processes including imperfections in the image segmentation process or occlusions. We assume that the detection errors operate independently on the

nodes of the graphs. As a result uncorrupted edges occur with total probability mass $(1-p)^2$. This probability mass is distributed between the $|E|$ edges of the graph. Edges with one node present and one-node missing have total probability mass $2p(1-p)$. This probability mass is distributed amongst the $2|V|$ configurations involving a node and a null-symbol ϵ . Edges in which both nodes are missed take the remaining probability mass, i.e. p^2 . There is one such configuration i.e. (ϵ, ϵ) to which this mass of probability may be assigned.

When the two graphs to be matched are considered together, then there are nine cases in which the assigned probability is non-zero. We assume that joint errors in the two graphs under consideration are independent. Hence, the probabilities are taken in product. If p_M and p_D are the node detection error probabilities for the model and data graphs, then the distribution of joint probability for the transitions on the edit lattice is specified by the following rule

$$P(\gamma_k, \gamma_{k+1}) = \begin{cases} \frac{(1-p_D)^2 (1-p_M)^2}{|E_D| |E_M|} & \text{if } (a, c) \in E_D \text{ and } (b, d) \in E_M \\ \frac{(1-p_D)^2 p_M(1-p_M)}{|E_D| |V_M|} & \text{if } (a, c) \in E_D \text{ and } (b, d) \in (V_M \times \epsilon) \cup (\epsilon \times V_M) \\ \frac{(1-p_D)^2 p_M^2}{|E_D|} & \text{if } (a, c) \in E_D \text{ and } (b, d) = (\epsilon, \epsilon) \\ \frac{p_D(1-p_D)^2 (1-p_M)^2}{|V_D| |E_M|} & \text{if } (a, c) \in (V_D \times \epsilon) \cup (\epsilon \times V_D) \text{ and } (b, d) \in E_M \\ \frac{p_D(1-p_D)^2 p_M(1-p_M)}{|V_D| |V_M|} & \text{if } (a, c) \in (V_D \times \epsilon) \cup (\epsilon \times V_D) \text{ and } (b, d) \in (V_M \times \epsilon) \cup (\epsilon \times V_D) \\ \frac{p_D(1-p_D)^2 p_M^2}{|V_D|} & \text{if } (a, c) \in (V_D \times \epsilon) \cup (\epsilon \times V_D) \text{ and } (b, d) = (\epsilon, \epsilon) \\ p_D^2 \frac{(1-p_M)^2}{|V_M|} & \text{if } (a, c) = (\epsilon, \epsilon) \text{ and } (b, d) \in E_M \\ p_D^2 \frac{p_M(1-p_M)}{|V_M|} & \text{if } (a, c) = (\epsilon, \epsilon) \text{ and } (b, d) \in (V_M \times \epsilon) \cup (\epsilon \times V_M) \\ p_D^2 p_M^2 & \text{if } (a, c) = (\epsilon, \epsilon) \text{ and } (b, d) = (\epsilon, \epsilon) \\ 0 & \text{otherwise} \end{cases} \quad (18)$$

The single-site priors are found by summing the joint priors i.e. $P(\gamma_k) = \sum_{\gamma_{k+1}} P(\gamma_k, \gamma_{k+1})$,

and are given by

$$P(\gamma_k) = \begin{cases} \frac{(1-p_D)}{|V_D|} \frac{(1-p_M)}{|V_M|} & \text{if } a \in V_D \text{ and } b \in V_M \\ \frac{(1-p_D)}{|V_D|} p_M & \text{if } a \in V_D \text{ and } b = \epsilon \\ p_D \frac{(1-p_M)}{|V_M|} & \text{if } a = \epsilon \text{ and } b \in V_M \\ p_D p_M & \text{if } a = \epsilon \text{ and } b = \epsilon \end{cases} \quad (19)$$

As a result of these distribution rules, and under the assumption that the error process acts independently in the two graphs being matched, it can be shown that the quantity $R_{k,k+1}$ depends only of the edge densities $\rho_D = \frac{|V_D|^2}{E_D}$ and $\rho_M = \frac{|V_M|^2}{E_M}$ for the two graphs under study. The contingency table given can be expressed in terms of the transitions on the edit lattice. The move contingency table is

$$R_{k,k+1} = \begin{cases} \rho_M \rho_D & \text{if } \gamma_k \rightarrow \gamma_{k+1} \text{ is a diagonal transition on the edit lattice,} \\ & \text{i.e. } (a, c) \in E_D \text{ and } (b, d) \in E_M \\ \rho_M & \text{if } \gamma_k \rightarrow \gamma_{k+1} \text{ is a horizontal transition on the edit lattice,} \\ & \text{i.e. } (a, c) \in E_D \text{ and } b = \epsilon \text{ or } d = \epsilon \\ \rho_D & \text{if } \gamma_k \rightarrow \gamma_{k+1} \text{ is a vertical transition on the edit lattice,} \\ & \text{i.e. } a = \epsilon \text{ or } c = \epsilon \text{ and } (b, d) \in E_M \\ 1 & \text{if } a = \epsilon \text{ or } c = \epsilon \text{ and } b = \epsilon \text{ or } d = \epsilon \end{cases} \quad (20)$$

The node detection probabilities are cancelled-out between the numerator and denominator, and as a result the edge-compatibility coefficients are determined only by the edge densities in the two graphs being matched.

4.2 A Posteriori Correspondence Probabilities

The second model ingredient is the *a posteriori* probability of visiting a site on the lattice. To motivate our model, we draw on matrix perturbation theory [38]. It can be shown that the change in the leading eigenvector depends in a linear manner on the perturbations in the elements of the adjacency matrix [30]. Moreover, in prior work, we have shown that a Bernoulli distribution can be successfully used to model noise in the elements of the adjacency

matrix [28]. As a result, if the matrix is large (i.e. the change in the leading eigenvector is the result of the sum of a large number of adjacency matrix element perturbations), then, as a consequence of the central limit theorem, the distribution of errors in the leading eigenvector due to perturbations in the elements of the adjacency matrix will be Gaussian. In other words we can write,

$$P(\gamma_k | \phi_X^*(a), \phi_Y^*(b)) = \begin{cases} \frac{1}{\sqrt{2\pi}\sigma} \exp\left\{-\frac{1}{2\sigma^2}(\phi_X^*(a) - \phi_Y^*(b))^2\right\} & \text{if } a \neq \epsilon \text{ and } b \neq \epsilon \\ \alpha & \text{if } a = \epsilon \text{ or } b = \epsilon \end{cases} \quad (21)$$

where σ^2 is the noise variance for the components of the leading eigenvectors. The perturbation argument does not deal with the more intractable problem of modelling changes in the size of the matrix (i.e. possible node insertions and deletions). In addition, it is worth mentioning that there are alternatives to measuring the difference in the eigenvectors using the L2 norm between eigenvectors in the probability distribution function. For instance, error could be measured by the angle between eigenvectors making use of a Von Mises distribution [24].

4.3 Minimum Cost Path

Once the edit costs are computed, we proceed to find the path that yields the minimum edit distance. Our adopted algorithm makes use of the fact that the minimum cost path along the edit lattice is composed of sub-paths that are also always of minimum cost. Hence, following Levenshtein [19] we compute a $|V_D| \times |V_M|$ transition-cost matrix ψ . The elements of the matrix are computed recursively using the formula

$$\psi(i, j) = \begin{cases} \eta(\gamma_i \rightarrow \gamma_j) & \text{if } j = 1 \text{ and } i = 1 \\ \eta(\gamma_i \rightarrow \gamma_j) + \psi_{i,j-1} & \text{if } i = 1 \text{ and } j \geq 2 \\ \eta(\gamma_i \rightarrow \gamma_j) + \psi_{i-1,j} & \text{if } j = 1 \text{ and } i \geq 2 \\ \eta(\gamma_i \rightarrow \gamma_j) + \min(\psi_{i-1,j}, \psi_{i,j-1}, \psi_{i-1,j-1}) & \text{if } i \geq 2 \text{ and } j \geq 2 \end{cases} \quad (22)$$

The matrix ψ is a representation of the accumulated minimal costs of the path along the edit lattice constrained to horizontal, vertical and diagonal transitions between adjacent

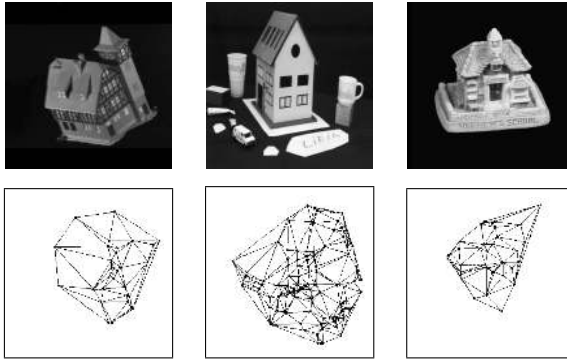


Figure 2: Example images and associated Delaunay triangulations.

coordinates. The minimum cost path can be proven to be that of the path closest to the diagonal of the matrix [19]. As a result, the edit distance is given by the bottom rightmost element of the transition-cost matrix. Hence, $d(X, Y) = \psi(|V_D|, |V_M|)$.

At this point it is worth commenting on the complexity of the seriation method. First, the leading eigenvector of the adjacency matrix needs to be computed. For a $N \times N$ adjacency matrix, there are numerical methods that can recover the eigenvalues and eigenvectors with complexity $O(N^3)$. However, the leading eigenvector can be computed with complexity $O(N^2)$ using the power method [13]. Second, we need to search for the seriation path of the average degree of the graph is D , then the cost of this step is $O(N(D - 1))$. Finally, the minimum cost edit path needs to be recovered. If the longer string being matched is of length N and the shorter one of length M , then the complexity of this step is $O(NM^2)$.

5 Experiments

Our experimental study is concerned with demonstrating the utility of the distances computed using our new method for the problem of graph-clustering. We explore three real-world problems. The first of these involves a database containing different views of a number of 3D objects. The second application involves view-based object recognition from 2D views of 3D objects using topographic information furnished using shape-from-shading. The third

problem involves finding sets of similar shapes in a database of trademarks and logos ¹.

5.1 View-based Object Recognition

We have experimented with our new matching method on an application involving a database containing different perspective views of a number of 3D objects. The objects used in our study are model houses. The different views are obtained as the camera circumscribes the object. The three object sequences used in our experiments are the CMU-VASC sequence, the INRIA MOVI sequence and a sequence of views of a model Swiss chalet. In our experiments we use ten images from each of the sequences. To construct graphs for the purposes of matching, we have first extracted corners from the images using the corner detector of Luo, Cross and Hancock [21]. The graphs used in our experiments are the Delaunay triangulations of these corner points. Our reason for using the Delaunay graph, is that of the point neighbourhood graphs (k-nearest neighbour graph, Gabriel graph, relative neighbourhood graph) it is the one that is least sensitive to node deletion errors [39]. Example images from the sequences and their associated Delaunay are shown in Figure 2. In Table 1 we list the numbers of nodes in the graphs and their edge densities. The table is divided into three blocks. Each block is for a different image sequence. The top row in each block shows the sequence number for the images.

5.1.1 Clustering

For the 30 graphs contained in the database, we have computed the complete set of $30 \times 29 = 870$ distances between each of the distinct pairs of graphs. We compare our results with those obtained when using the distances computed using two alternative methods. The first of these is the negative log-likelihood function computed using the EM algorithm reported by Luo and Hancock [22]. In this work the similarity of the graphs is gauged by the quantity $Tr[A_D^T Q M Q^T]$ where A_D is the $|V_D| \times |V_D|$ data-graph adjacency matrix, A_M is the $|V_M| \times |V_M|$ model graph adjacency matrix and Q is a $|V_D| \times |V_D|$ matrix of correspondence

¹All trademarks and logotypes remain the property of their respective owners. All trademarks and registered trademarks are used strictly for educational and academic purposes and without intent to infringe on the mark owners.

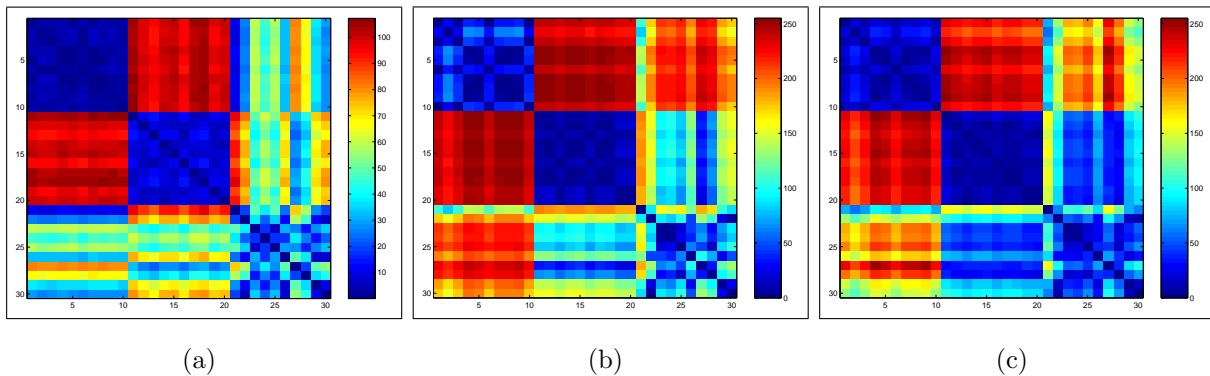


Figure 3: Edit distance matrices.

probabilities between the nodes of the data-graph and the model-graph. Maximum likelihood matches are found by performing singular value decomposition on the weighted correlation matrix $A_D^T Q A_M$ between the data-graph adjacency matrix and the model-graph adjacency matrix. This similarity measure uses purely structural information. The method hence shares with our edit distance framework the use of a statistical method to compare the eigenvector structure of two adjacency matrices. However, unlike our method which uses only the leading eigenvector of the adjacency matrix, this method uses the full pattern of singular vectors. In addition, the method is an iterative one which alternates between computing singular vectors in the M or maximisation step and re-computing the correspondence probability matrix Q in the E or expectation step. The second of the distance measures is computed using a spectral embedding of the graphs [23]. The method involves embedding the graphs in a pattern space spanned by the leading eigenvalues of the adjacency matrix. According to this method, the distance between graphs is simply the L2 norm between points in this pattern space [23]. This pairwise graph similarity measure again shares with our new method the feature of using spectral properties of the adjacency matrix.

In Figure 3a we show the distance matrix computed using our algorithm. The similarity matrix obtained using the method of Luo and Hancock [23] is shown in Figure 3b, while the distance matrix computed from the spectral embedding is shown in Figure 3c. In each distance-matrix the element with row column indices i, j corresponds to the pairwise similarity between the graph indexed i and the graph indexed j in the database. In each matrix the

graphs are arranged so that the row and column index increase monotonically with viewing angle. The blocks of views for the different objects follow one another. The darker the entry, the smaller the distance. From the matrices in Figure 3, it is clear that the different objects appear as distinct blocks. Within each block, there is substructure (sub-blocks) which correspond to different characteristic views of the object. The main feature to note from the three matrices is that there is less confusion between the third block (Chalet sequence) and the first two blocks (CMU and MOVI sequences), when our edit-distance method is used.

For visualisation purposes, we have performed multidimensional scaling (MDS) on the pairwise distance matrices to embed the graphs in an eigenspace. Broadly speaking, this is a method for visualising objects characterised by pairwise distance rather than by ordinal values. It hinges around computing the eigenvectors of a similarity matrix, The leading components of the eigenvectors are the coordinates associated with the graphs. The method can be viewed as embedding the graphs in a pattern space using a measure of their pairwise similarity to one another. It is interesting to note that when the distance measure used is the L2 norm, then MDS is equivalent to principal components analysis. However, with graph edit distance this is not the case. We plot the positions of the graphs on the plane corresponding to the two leading dimensions of the resulting eigenspace. We construct the embeddings using the entire similarity matrix for the three different objects, with the aim of determining whether the eigenspace captures the structural differences between the sets of graphs for the distinct objects in our experimental data-set. In Figure 4, from left to

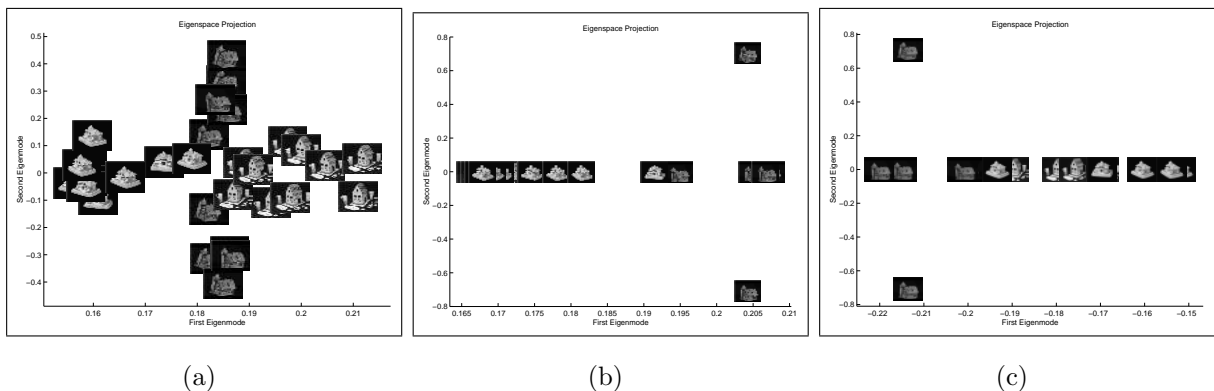


Figure 4: Eigenspace projections for each of the distance matrices used.

right, we show the embeddings corresponding to the distance matrices computed using our algorithm, the negative log-likelihood computed using the algorithm of Luo and Hancock [23] and the spectral feature-vectors extracted from the adjacency matrix [23]. Of the three distance measures, the clusters resulting from the use of the edit distance described in this paper produce the clearest cluster structure. Hence our new distance measure appears to be effective at distinguishing between different classes of object.

Based on the visualisation provided by MDS, it appears that the distances furnished by our edit-distance method may be suitable for the purposes of graph-clustering. We have therefore applied a pairwise clustering algorithm to the similarity data for the graphs. The process of pairwise clustering is somewhat different to the more familiar one of central clustering. Whereas central clustering aims to characterise cluster-membership using the cluster mean and variance, in pairwise clustering it is the relational similarity of pairs of objects which are used to establish cluster membership. Although less well studied than central clustering, there has recently been renewed interest in pairwise clustering aimed at placing the method on a more principled footing using techniques such as mean-field annealing [14]. In this paper we apply the pairwise clustering algorithm of Robles-Kelly and Hancock [28] to the similarity data for the complete database of graphs. Our aim is to determine which distance measure results in a cluster assignment which best corresponds to the three image sequences. The pairwise clustering algorithm requires distances to be represented by a matrix of pairwise affinity weights. Ideally, the smaller the distance, the stronger the weight, and hence the mutual affinity to a cluster. The affinity weights are required to be in the interval $[0, 1]$. For the pair of graphs indexed $i1$ and $i2$ the affinity weight is taken to be

$$W_{i1,i2}^{(0)} = \exp\left(-k \frac{d(i1, i2)}{\max_{i1,iq}(d(i1, iq))}\right) \quad (23)$$

where k is a constant and $d(i1, i2)$ is the edit distance between the graph indexed $i1$ and the graph indexed $i2$. The clustering algorithm is described in detail in [28] and is summarised in the supplementary electronic material. It is an iterative process. The process maintains two sets of variables. The first of these is a set of cluster membership indicators $s_{i\omega}^{(n)}$ which measures the affinity of the graph indexed i to the cluster indexed ω at iteration n of the

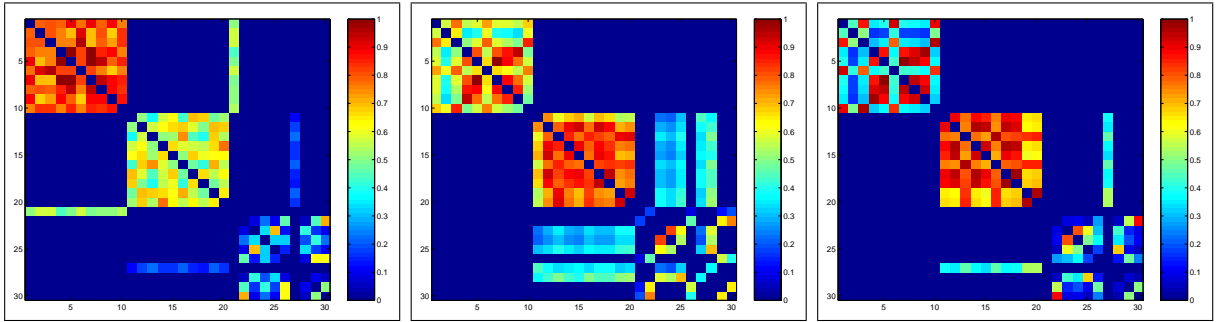
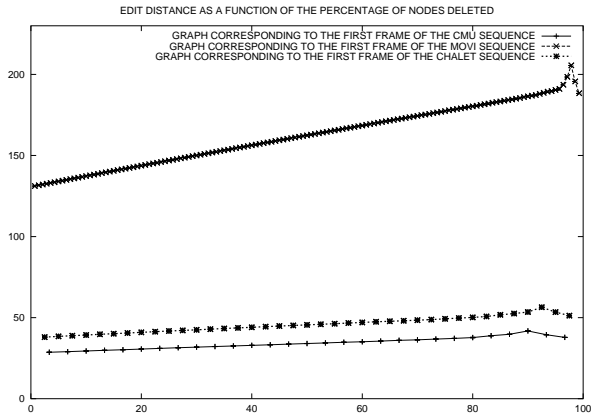


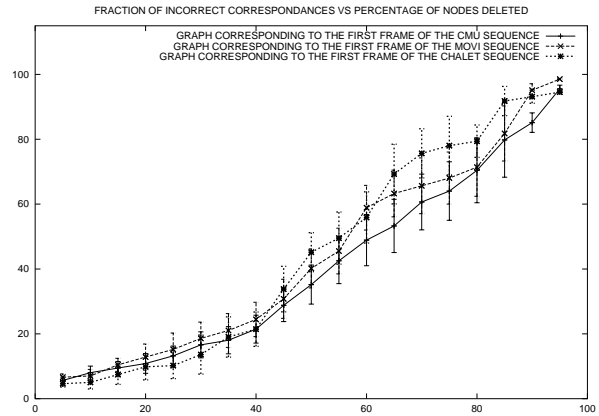
Figure 5: Final similarity matrices for the clustering process.

algorithm. The second, is an estimate of the affinity matrix based on the current cluster-membership indicators $W^{(n)}$. These two sets of variables are estimated using interleaved update steps, which are formulated to maximise a likelihood function for the pairwise cluster configuration.

The final similarity matrices generated by the clustering process for each of the distance measures studied are shown in Figure 5. From left-to-right, the panels show the similarity matrices obtained using our edit distance, the Luo and Hancock structural graph matching algorithm (SGM), and the spectral feature vectors. The lighter the entries, the more similar the corresponding pairs of graphs. Ideally, the clusters should appear as square blocks centred along the diagonal of the matrices. The misassignment of graphs to clusters is characterised by strong response outside these blocks. In the case of our edit distance, the first and seventh graphs in the third block (i.e. the Chalet sequence) are respectively misassigned to the first block (the CMU sequence) and the second block (the MOVI sequence). In the case of the spectral feature vectors, four of the Chalet sequence graphs are misassigned to the MOVI sequence. In the case of Luo and Hancock method, only the seventh Chalet graph is misassigned to the MOVI cluster. The errors are due to the fact that the graphs in question are morphologically more similar to the graphs in the CMU and MOVI sequences than to those in the Chalet sequence. Our method compares favourably when computational cost is taken into account. This is because our method only requires the computation of the leading eigenvector while the spectral feature vectors require the complete eigenstructure to be computed. In consequence, the edit distance takes on average a factor of 2.6 less



(a) Edit distance vs nodes deleted



(b) Correspondance error vs nodes deleted

Figure 6: Structural sensitivity plots

time to compute than the spectral feature vectors. Since the complexity of the eigenvector component of the method presented in this paper is $O(N^2)$ while that for the Luo and Hancock method is $O(N^3)$, this difference can be expected to grow with increasing graph size.

CMU	1	2	3	4	5	6	7	8	9	10
Number of Nodes	30	32	32	30	30	32	30	30	30	31
Edge Density	5.6	5.2	4.9	4.8	5.5	5.6	5.7	5.6	5.4	5.4
MOVI	11	12	13	14	15	16	17	18	19	20
Number of Nodes	140	134	130	136	137	131	139	141	133	136
Edge Density	6.4	6.8	6.6	6.5	6.7	6.8	7.1	7.2	6.9	7.4
Chalet	21	22	23	24	25	26	27	28	29	30
Number of Nodes	40	57	92	78	90	64	113	100	67	59
Edge Density	5.9	5.6	5.9	6.0	5.9	6.2	6.1	6.3	5.9	6.1

Table 1: Image statistics.

5.1.2 Structural Sensitivity to Node Deletion Error

We have conducted some experiments to measure the sensitivity of our matching method to structural differences in the graphs and to provide comparison with alternatives. Here we have taken the first graph from each of the three sequences described above. We have simulated the effects of structural errors by randomly deleting nodes and re-triangulating the remaining point-set. To demonstrate the effect of these structural errors, in Figure 6a we show the edit distance as a function of the number of deleted nodes. We have averaged the edit distance over 10 different sets of random node deletions. The different curves in the plot are for the different seed graphs. In each case the edit distance varies almost linearly with the number of deleted nodes. The deviations from the linear dependence occur when large fractions of the graph are deleted.

To investigate the effect of node detection errors, in Figure 6b we show the fraction of correspondence errors as a function of the fraction of nodes deleted from the graphs. Here, we consider the model graph to be the initial graph, i.e. the deletion-free Delaunay triangulation. The main features to note from this plot are as follows. First, the fraction of correspondence errors is always lower than the fraction of deleted nodes. Second, there appears to be no systematic effect of varying the graph size.

Finally, we investigated the effect of the node deletion errors on the results of MDS. In Figure 7 we show the distance matrix (left-hand panel) and the MDS embedding (right-hand panel) for the graphs. The graphs belonging to the different noise perturbed sets are denoted by different characters, and form well defined clusters. Hence, structural (node deletion errors) do not appear to affect adversely the clustering process.

5.2 Constant Shape Index Maximal Patches

Our second real world example is also concerned with view-based object recognition. Here we have used the COIL database which consists of a series of 2D views of 3D objects collected at 72 equally spaced viewing directions on a great circle of the object view-sphere. To extract graphs from the object-views, we have proceeded as follows. We first apply shape-from-shading [45] to the object views to extract fields of surface normals. From the fields of surface

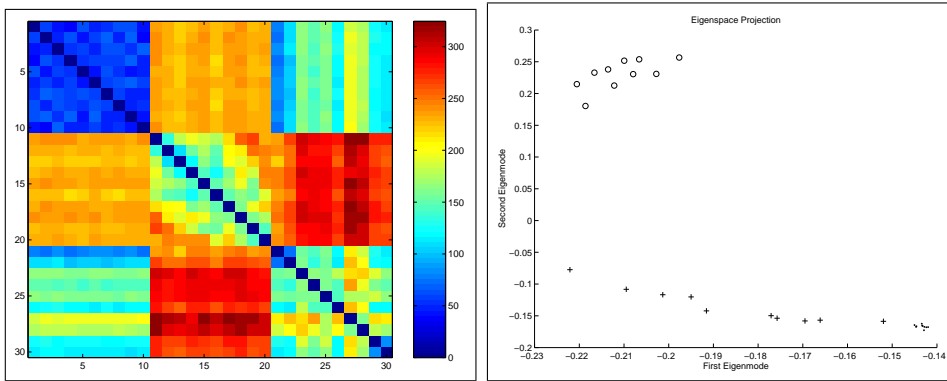


Figure 7: Distance matrix and MDS plot for our set of random graphs.

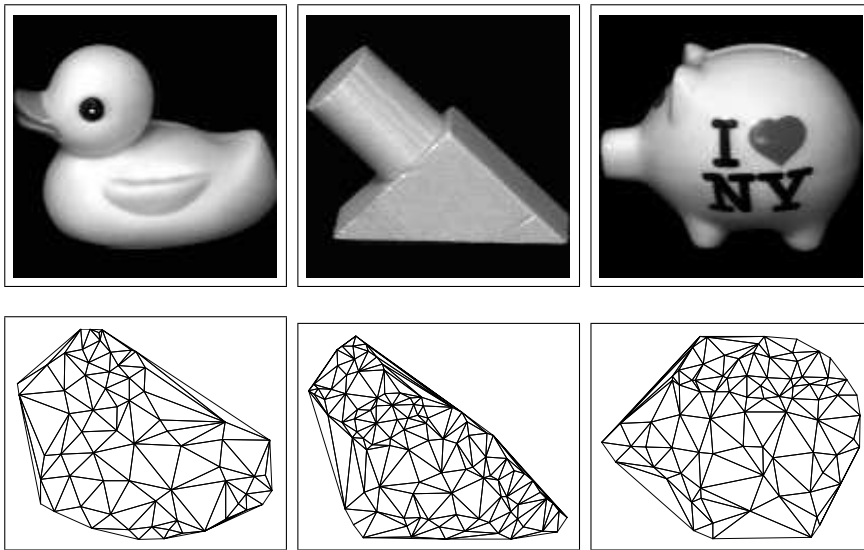


Figure 8: Example views and graphs for the three COIL objects used in our experiments.

normals we follow Dorai and Jain [9] and compute the Koenderink and Van Doorn shape-index [18]. The shape-index is a curvature invariant measure of local surface topography that distinguishes smoothly between ridges, ravines, saddles, domes and cups using an angular descriptor. The object views are segmented into regions of uniform shape-index (constant shape-index maximal patches or CSMP's). For the arrangement of CSMP's we compute the region adjacency graph. We have computed edit distances between the graphs and have subjected the distances to multidimensional scaling.

In our experiments, we have used three objects and ten views for each object. Figure 8

shows some example views and the corresponding graphs. In Figure 9, we show the result of applying MDS to the graph edit distances. The left-most panel shows the three object clusters, which are well separated. The remaining panels show magnified views of the clusters for the individual objects. The different views of the three objects are well separated and form distinct clusters. This feature of the data is supported in Figure 10 where from left-to-right the panels show the raw edit distance matrix, the matrix of initial graph similarities, and the matrix of final graph similarities. Despite the fact that there is overlap in the block of the initial similarity matrix, in the final similarity matrix the cluster blocks are cleanly separated and none of the object-views is misassigned.

5.3 Database of Logo's

The third application involves using the clustering methods outlined in the previous section for image database indexing and retrieval. As proof of concept, we have performed experiments on a relatively small database containing 245 binary images of trademark-logos used previously in the study of Huet and Hancock [16]. Here, the graphs are constructed as follows. First, we apply the Canny edge detector [5] to the images to extract connected edge-chains. A polygonalisation procedure [27] is applied to the edge-chains to locate straight line segments. For each line-segment, we compute the centre-point. The graphs used in our experiments are the Delaunay triangulations of the line-centres. In the top left-hand-panel in Figure 11, we show an example of the images used in our experiments. The middle panel shows the results of the line-segment extraction step. The corresponding Delaunay graph is displayed in the right-hand-panel. For each pair of Delaunay graphs we compute the edit-

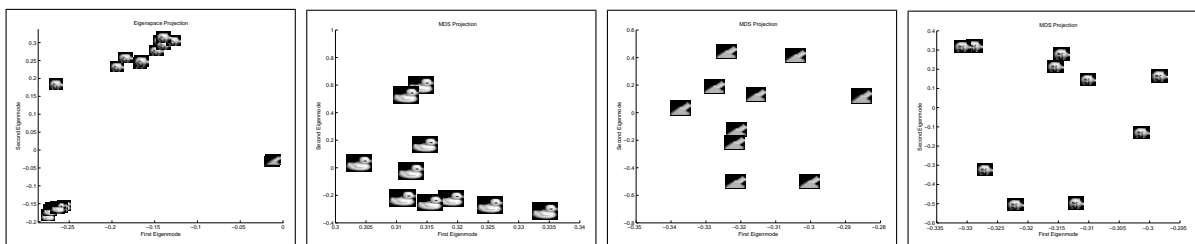


Figure 9: MDS results for the COIL objects used in our experiments.

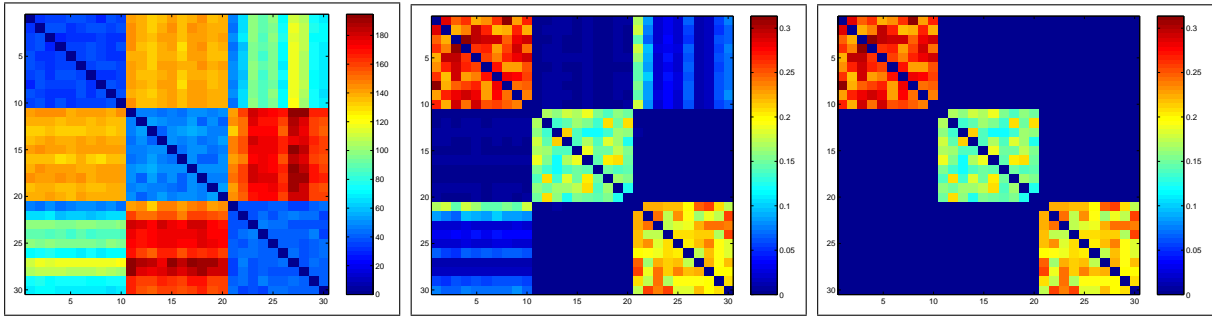


Figure 10: Distance matrix and initial and final affinity matrices for the objects in the COIL database used in our experiments.

distance. We have again applied both multidimensional scaling and pairwise clustering to the distance matrix.

Turning our attention first to the results of multidimensional scaling Figure 12 shows the distribution of graphs in the space spanned by the leading two eigenvectors of the similarity matrix. The graphs are distributed along an annulus. Analysis of the data shows that the position along the length of the annulus corresponds to the size (i.e. number of nodes) of the graphs, while the position away from it depends on the variation in structure for graphs of the same size.

Next, we turn our attention to the results of applying pairwise clustering to the set of edit distances for the logos. We obtained 34 clusters, with an average of 7 images per cluster.

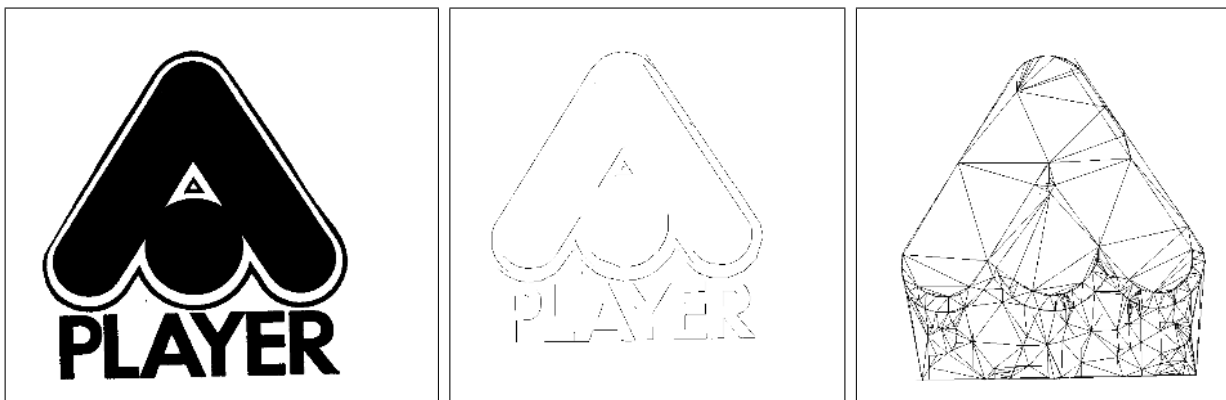


Figure 11: Example image, polygonalisation results and Delaunay triangulation

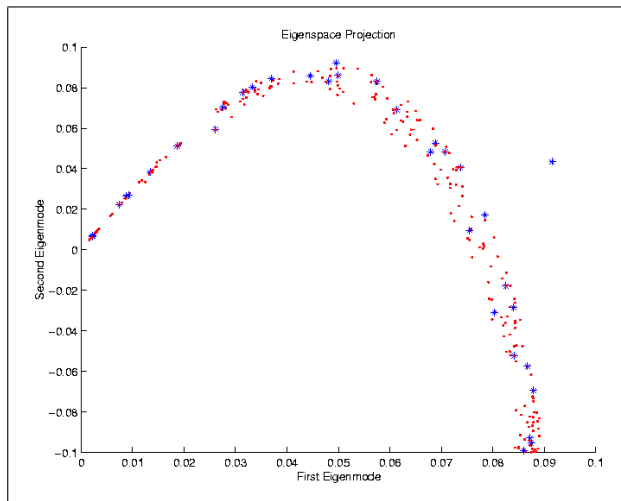


Figure 12: Multidimensional scaling applied to the matrix of edit distances for the logos.

To display the results, we find the modal graph for each cluster. For the cluster indexed ω the modal graph has the largest cluster-membership indicator $s_{i\omega}^{(\infty)}$ at convergence of the clustering process. In other words it is the graph with index $i_{\omega}^* = \arg \max_i s_{i\omega}^{(\infty)}$. We then rank the remaining graphs in the order of their increasing distance from the modal graph for the cluster ω . The significance of the cluster indexed ω is gauged by the total mass of membership indicator $m_{\omega} = \sum_{i \in \Omega} s_{i\omega}^{(\infty)}$. In Figure 13, the different rows show the images belonging to the eight most significant clusters. The left-most image in each row is the image corresponding to the modal graph for the cluster. The subsequent images in each row correspond to the most similar graphs in order of increasing edit distance. It is interesting to note that similar logos appear in the same cluster. For instance, the two “Crush” logos (one with a palm-tree and one with a fruit-segment) appear in the top row, the “Hotel Days”, “Auberge Daystop” and “Les Suites Days” appear in the second row, and, the two “Incognito” logos in the third row. However, the clusters do not seem to correspond to obvious shape categories. Hence, it would appear that we need to exploit the distances in a more sophisticated shape indexation procedure.

To this end, we note that once the database has been clustered, then we can use the cluster structure in the search for the most similar object. The idea is to find the cluster whose modal graph is most similar to the query. The graph within the cluster that is most

similar to the query is the one that is retrieved. The search process is as follows. Suppose the query graph is denoted by G_q . First, we compute the set of graph edit distances between the graph G_q and the modal graphs for each cluster. The distance between the graph G_q and the modal graph for the cluster ω is denoted by $d_{q\omega}^*$. The cluster with the most similar modal graph is $\omega_q = \arg \min_{\omega} d_{q\omega}^*$. We search the graphs in this cluster to find the one that is most similar to the query graph. The set of graphs belonging to the cluster ω_q is $C_q = \{i | s_{i\omega_q}^{(\infty)} = \arg \max_{\omega} s_{i\omega}^{(\infty)}\}$. The retrieved graph is the member of the set C_q which has the minimum edit distance to the query graph G_q , i.e. the one for which $i_q = \arg \min_{i \in C_q} d_{qi}$. It must be stressed that this simple recall strategy is presented here just to illustrate that the edit distances can be used to cluster images and organise the database. The information retrieval literature contains more principled and more efficient alternatives which should be used if the example given here is scaled to very large databases of thousands or tens of thousands of images.

In Figure 14, we show the results of three query operations. The top image in each column shows the query image and the subsequent images correspond to the retrieved images in order of increasing graph edit distance. In the left-hand column we show the result of querying with the ‘‘Auberge Daystop’’ logo. The two most similar images have the same shape, but carry the legends ‘‘Hotel Days’’ and ‘‘Les Suites Days’’. The middle row shows the result of querying with the ‘‘Incognito-plus’’ logo, which returns the ‘‘Incognito-cotton’’ logo as the most similar graph. In the right-hand column we show the result of querying with the ‘‘Crush’’ logo. Here the most similar graph again contains the ‘‘Crush’’ legend, but the orange segment is replaced by a palm-tree. It is worth noting that the database contains only two logos of the ‘‘Days Inn’’ type and a single ‘‘Crush’’ and ‘‘Incognito’’ type image. Hence, from our results, we can conclude that the algorithm is able to cope with structural variations and differences in graph-size. Of course, this cluster-based retrieval method has its potential drawbacks. First, if logos are assigned to the wrong cluster, then the retrieval process will fail. This problem can be overcome if the search proceeds beyond the cluster with the best-match modal graph, to the N best matched clusters. The second problem is that of cluster merging or cluster fragmentation, which again mean that a more sophisticated



Figure 13: Left-hand column: Cluster-centers; Right-hand columns: Members of the cluster arranged according to their rank.



Figure 14: Top row: input query images; Bottom rows: search results.

search strategy is needed.

We have placed this study on a more quantitative basis by computing precision-recall curves for the retrieval method. Figure 15 shows the precision-recall curves for the three queries described above. It is the “Days-Inn” query that shows the fastest fall-off of precision with recall. In the case of the remaining two queries, the fall-off does not take place until the value of the recall is greater than 0.8.

6 Conclusions

The work reported in this paper provides a synthesis of ideas from spectral graph-theory and structural pattern recognition. We use a graph spectral seriation method based on

the leading eigenvector of the adjacency matrix to convert graphs to strings. We match the resulting string representations by minimising edit distance. The edit costs needed are computed using a simple probabilistic model of the edit transitions, which is designed to preserve the edge order on the correspondences. The minimum cost edit sequence may be used to locate correspondences between nodes in the graphs under study. We have also demonstrated that the edit distances can be used to cluster graphs into meaningful classes.

There are a number of ways in which the work described in this paper may be extended. First, although we have concentrated on unweighted graphs, it would be interesting to extend it to weighted graphs. Second, there are alternative ways of computing the minimum cost edit sequence, and these may improve both the efficiency and accuracy of the method. One recently developed method that would be interesting to explore in this context are string-kernels.

References

- [1] J. E. Atkins, E. G. Bowman, and B. Hendrickson. A spectral algorithm for seriation and the consecutive ones problem. *SIAM Journal on Computing*, 28(1):297–310, 1998.
- [2] A. D. Bagdanov and M. Worring. First order gaussian graphs for efficient structure classification. *Pattern Recognition*, 36(6):1311–1324, 2003.

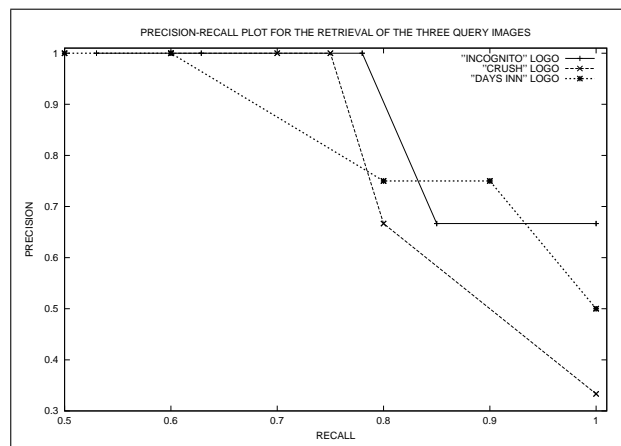


Figure 15: Precision-recall plots for the database of trademark logos.

- [3] H. Bunke. On a relation between graph edit distance and maximum common subgraph. *Pattern Recognition Letters*, 18(8):689–694, 1997.
- [4] H. Bunke, A. Munger, and X. Jiang. Combinatorial search vs. genetic algorithms: A case study based on the generalized median graph problem. *Pattern Recognition Letters*, 20(11-13):1271–1279, 1999.
- [5] J. Canny. A computational approach to edge detection. *IEEE Trans. on Pattern Analysis and Machine Intelligence*, 8(6):679–698, 1986.
- [6] W. J. Christmas, J. Kittler, and M. Petrou. Structural matching in computer vision using probabilistic relaxation. *IEEE Transactions on Pattern Analysis and Machine Intelligence*, 17(8):749–764, 1995.
- [7] Fan R. K. Chung. *Spectral Graph Theory*. American Mathematical Society, 1997.
- [8] E. W. Dijkstra. A note on two problems in connection with graphs. *Numerische Math*, 1:269–271, 1959.
- [9] C. Dorai and A.K. Jain. Shape spectrum-based view grouping and matching of 3d free-form objects. *EEE Trans. Pattern Analysis and Machine Intelligence*, 19(10):1139–1145, 1997.
- [10] M. A. Eshera and K. S. Fu. A graph distance measure for image analysis. *IEEE Transactions on Systems, Man and Cybernetics*, 14:398–407, 1984.
- [11] A. M. Finch, R. C. Wilson, and E. R. Hancock. An energy function and continuous edit process for graph matching. *Neural Computation*, 10(7):1873–1894, 1998.
- [12] S. Gold and A. Rangarajan. A graduated assignment algorithm for graph matching. *PAMI*, 18(4):377–388, April 1996.
- [13] G. H. Golub and C. F. Van Loan. *Matrix Computations*. The Johns Hopkins Press, 1996.
- [14] T. Hofmann and M. Buhmann. Pairwise data clustering by deterministic annealing. *IEEE Transactions on Pattern Analysis and Machine Intelligence*, 19(1):1–14, 1997.
- [15] R. Horaud and H. Sossa. Polyhedral object recognition by indexing. *Pattern Recognition*, 28(12):1855–1870, 1995.

- [16] B. Huet and E. R. Hancock. Relational object recognition from large structural libraries. *Pattern Recognition*, 35(9):1895–1915, 2002.
- [17] J. Keuchel, C. Schnorr, C. Schellewald, and D. Cremers. Binary partitioning, perceptual grouping, and restoration with semidefinite programming. *IEEE Trans. on Pattern Analysis and Machine Intelligence*, 25(11):1364–1379, 2003.
- [18] J. J. Koenderink and A. J. van Doorn. Surface shape and curvature scales. *Image and Vision Computing*, 10(8):557–565, 1992.
- [19] V. I. Levenshtein. Binary codes capable of correcting deletions, insertions and reversals. *Sov. Phys. Dokl.*, 6:707–710, 1966.
- [20] L. Lovász. Random walks on graphs: a survey. *Bolyai Society Mathematical Studies*, 2(2):1–46, 1993.
- [21] Bin Luo, A. D. J. Cross, and E. R. Hancock. Corner detection via topographic analysis of vector-potential. *Pattern Recognition Letters*, 20(6):635 – 650, 1999.
- [22] Bin Luo and E. R. Hancock. Structural graph matching using the EM algorithm and singular value decomposition. *IEEE Trans. on Pattern Analysis and Machine Intelligence*, 23(10):1120–1136, 2001.
- [23] Bin Luo, R. C. Wilson, and E. R. Hancock. Spectral embedding of graphs. *Pattern Recognition*, 36:2213–2223, 2003.
- [24] K. V. Mardia and P. E Jupp. *Directional Statistics*. John Wiley & Sons, 2000.
- [25] B. Mohar. Some applications of laplace eigenvalues of graphs. In G. Hahn and G. Sabidussi, editors, *Graph Symmetry: Algebraic Methods and Applications*, NATO ASI Series C, pages 227–275, 1997.
- [26] R. Myers, R. C. Wilson, and E. R. Hancock. Bayesian graph edit distance. *PAMI*, 22(6):628–635, June 2000.
- [27] Yin Peng-Yeng. Algorithms for straight line fitting using k-means. *Pattern Recognition Letters*, 19:31–41, 1998.

- [28] A. Robles-Kelly and E. R. Hancock. A probabilistic spectral framework for spectral clustering and grouping. *Pattern Recognition*, 37(7):1387–1405, 2004.
- [29] A. Robles-Kelly and E. R. Hancock. String edit distance, random walks and graph matching. *Int. Journal of Pattern Recognition and Artificial Intelligence*, 18(3):315–327, 2004.
- [30] A. Robles-Kelly, S. Sarkar, and E. R. Hancock. A fast leading eigenvector approximation for segmentation and grouping. In *International Conference on Pattern Recognition*, pages I:639–642, 2002.
- [31] A. Sanfeliu and K. S. Fu. A distance measure between attributed relational graphs for pattern recognition. *IEEE Transactions on Systems, Man and Cybernetics*, 13:353–362, 1983.
- [32] G. Scott and H. Longuet-Higgins. An algorithm for associating the features of two images. In *Proceedings of the Royal Society of London*, number 244 in B, pages 21–26, 1991.
- [33] B. Selman, H. A. Kautz, and B. Cohen. Noise strategies for improving local search. In *Proc. of the Twelfth National Conference on Artificial Intelligence*, pages 337–343, 1994.
- [34] L. G. Shapiro and R. M. Haralick. Relational models for scene analysis. *IEEE Transactions on Pattern Analysis and Machine Intelligence*, 4:595–602, 1982.
- [35] L. S. Shapiro and J. M. Brady. A modal approach to feature-based correspondence. In *British Machine Vision Conference*, pages 78–85, 1991.
- [36] A. Shokoufandeh, S. J. Dickinson, K. Siddiqi, and S. W. Zucker. Indexing using a spectral encoding of topological structure. In *Proceedings of the Computer Vision and Pattern Recognition*, pages 491–497, 1998.
- [37] O. Steinmann, A. Strohmaier, and T. Stutzle. Tabu search vs. random walk. In *Advances in Artificial Intelligence (KI-97)*, pages 337–348, 1997.
- [38] G. W. Stewart and Ji-Guang Sun. *Matrix Perturbation Theory*. Academic Press, 1990.
- [39] M. Tuceryan and T. Chorzempa. Relative sensitivity of a family of closest-point graphs in computer vision applications. *Pattern Recognition*, 24(5):361–373, 1991.
- [40] S. Umeyama. An eigen decomposition approach to weighted graph matching problems. *PAMI*, 10(5):695–703, September 1988.

- [41] R. S. Varga. *Matrix Iterative Analysis*. Springer, second edition, 2000.
- [42] R. A. Wagner and M. J. Fisher. The string-to-string correction problem. *Journal of the ACM*, 21(1):168–173, 1974.
- [43] R. C. Wilson and E. R. Hancock. A bayesian compatibility model for graph matching. *Pattern Recognition Letters*, 17:263–276, 1996.
- [44] R.C. Wilson and E. R. Hancock. Structural matching by discrete relaxation. *IEEE Transactions on Pattern Analysis and Machine Intelligence*, 19(6):634–648, June 1997.
- [45] P. L. Worthington and E. R. Hancock. New constraints on data-closeness and needle map consistency for shape-from-shading. *IEEE Transactions on Pattern Analysis and Machine Intelligence*, 21(12):1250–1267, 1999.